Proceedings of the 1st Global Power and Propulsion Forum
GPPF 2017
Jan 16-18, 2017, Zurich, Switzerland
www.pps.global

GPPF-2017-0060

TIP GAP SIZE EFFECTS ON THERMAL PERFORMANCE OF CAVITY-WINGLET TIPS IN TRANSONIC TURBINE CASCADE WITH ENDWALL MOTION

Chao Zhou *
State Key Laboratory for Turbulence and Complex Systems, College of Engineering, Peking University
czhou@pku.edu.cn
Beijing, China

Fangpan Zhong
State Key Laboratory for Turbulence and Complex Systems, College of Engineering, Peking University
zhongfp@pku.edu.cn
Beijing, China

ABSTRACT

The thermal performance of two cavity-winglet tips with endwall motion is investigated in a transonic high pressure turbine cascade, which operates at an engine representative exit Mach number of 1.2 and an exit Reynolds number of 1.7×10^6. The numerical method is first validated with experimental data and then used to investigate blade heat transfer at three different tip clearances of 1.1%, 2.1% and 3.1% chord. The effects of relative endwall motion are considered. The present results show that as the size of the tip gap increases, the heat transfer coefficient and heat load on the tip increases. The winglet geometries on the blade tip mainly affect the tip flow structure close to them. At a larger tip clearance, the size of the separation bubble above the pressure side winglet increases. The heat transfer coefficient is high on the pressure side winglet due to the flow reattachment at all tip clearances. Within the tip gap, when the size of the tip clearance increases, the size of the cavity vortex increases and the cavity scraping vortex due to relative endwall motion becomes smaller. The impingement of the both two vortexes can lead to high heat transfer coefficient on the cavity floor surface. On the blade suction surface, when the size of the tip clearance increases, the heat transfer coefficient of the cavity tip increases, but those of the winglet tips decreases. The heat transfer coefficient is high on the side surface of the suction side winglet at all tip clearances because of the tip leakage flow impingement.

INTRODUCTION

In gas turbines, the tip clearance exists between the tip of turbine rotor blade and the stationary casing to prevent rubbing. The hot gas is driven across the blade tip due to the pressure difference between the blade pressure side and suction side, forming tip leakage flow. The tip leakage flow reduces the turbine efficiency and work output. According to Denton [1], the tip leakage loss could account for one third of the total aerodynamic loss of a turbine rotor.

Winglet tips were found to be able to reduce the tip leakage loss. A winglet refers to the extension part at the turbine tip region. It can be applied on a flat tip to form a flat-winglet tip or a squealer tip to form a squealer-winglet tip. The latter is preferred because many studies have shown that squealer tips can produce lower loss than the flat tips (Heyes et al. [1], Key and Arts [3], Lee and Kim [4]). With the additional design of winglets, the tip leakage loss of the squealer-winglet tip is believed to be lower than that of the flat-winglet tip. The aerodynamic performance of the squealer-winglet tip has been studied on both linear cascades (Schabowski et al. [5], Zhou et al. [6] and Cheon and Lee [7]) and rotating rigs (Harvey et al. [8]). In general, it was found that squealer-winglet tips performed better than the squealer tips.

Heat transfer is an important aspect for the tips of rotors in high pressure turbines. A review of turbine blade tip heat transfer is presented by Bunker [9]. A number of studies related to the flat tips or the squealer tips were published, e.g. Teng et al. [10], Bunker et al. [11], Kwak and Han [12], Azad et al. [13] and Newton et al. [14]. Fewer studies focus on the heat transfer of the squealer-winglet tips. Papa et al. [15] found that the squealer-winglet tip had lower average mass/heat transfer compared with the squealer tip. Saha et al. [16] found that the pressure side winglet reduced the tip average heat transfer coefficient by 1.5% on a suction-sided squealer tip. In a transonic turbine cascade, O'Dowd et al. [17] measured the heat transfer on winglet tip surface and near-tip side-walls of a unique squealer-winglet tip. Compared with the flat tip, they found a region of higher Nusselt number close to the tip on the suction surface. Nevertheless, the winglet tip geometries studied in different literatures are very different.

In a previous study by Zhong et al. [18], the heat transfer performance of three different cavity-winglet tips was investigated experimentally and numerically in a transonic turbine cascade at a tip clearance of 2.1% chord. It was found that the heat transfer coefficient was very high on the pressure side winglet due to the flow separation reattachment and also

* Corresponding author

quite high on the side surface of the suction side winglet due to the impingement of the tip leakage vortex. Their results also showed that the effect of endwall motion between the blade tip and casing was significant, which was also observed by other researchers, such as Tallman and Lakshminarayana [19], Yaras and Sjolander [20], Palafox et al. [21], Zhou [22], Rhee and Cho [23].

For a turbine, the size of the tip clearance varies and this effect changes the thermal performance of the tips. This paper presents a following work of Zhong et al. [18]. The aim is to understand the effect of tip clearance on the thermal performance of different winglet tips with endwall motion. In this study, two winglet tips and a baseline cavity tip are investigated at three tip clearances of 1.1%, 2.1% and 3.1% chord. The heat transfer on the tip and near tip surface are presented and the flow field is analysed to give explanations to the thermal performance of the blade tips.

COMPUTATIONAL DETAILS

Tip Geometry

The tip geometries are shown in Fig. 1. They are the same as those used in the previous study [18]. The width and height of the cavity squealer are 2.6% chord and 5.1% chord respectively. The winglet tip 'SSW' has a suction side fore-part winglet between $0.15C_x$ and $0.62C_x$. The winglet tip 'PSW' has the same suction side winglet as "SSW" and a pressure side winglet. The design of the suction side winglet is based on the method proposed by Zhou and Zhong [24]. The cascade profile is the blade geometry near the tip of a modern transonic high pressure turbine rotor. The main parameters of the cascade are listed in Table 1.

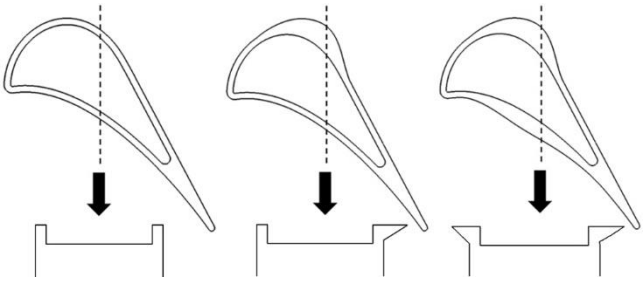

(a) Cavity (b) SSW (c) PSW

Fig. 1 Tip geometries

Blade Inlet Angle (β_1)	45.0°
Blade Exit Angle (β_2)	-57.0°
Chord (C)	46.8 mm
Axial Chord (C_x)	39.2 mm
Span (H)	43.0 mm
Pitch (t)	37.9 mm

Table 1 Main parameters of the cascade

Meshing and Computational Solver

Fig. 2 shows the computational domain and mesh of the cavity tip. The computational domain uses one blade with periodic boundary conditions to simulate a row of blades. The inlet of the computational domain is located 0.3 axial chord upstream of the cascade and the domain outlet is located 1.2 axial chord downstream of the cascade.

The meshes are built with commercial software ICEM CFD. All of the meshes are structured hexahedral with mesh growth factor less than 1.3. The tip average y+ is around 2.

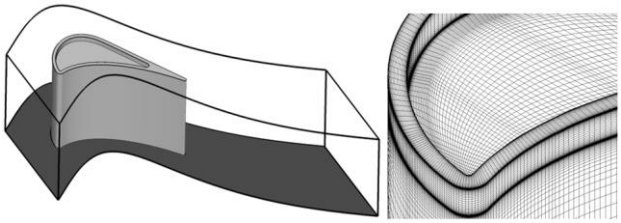

Fig. 2 Computational domain and mesh of the cavity tip

The Commercial software ANSYS Fluent is employed to solve the steady Reynolds-averaged Navier-Stokes (RANS) equations, which are discretized in space using a second order. The turbulence model is Spalart-Allmaras (SA) model. The 'pressure inlet' and 'pressure outlet' conditions are applied to the inlet and outlet of the computational domain. For each case, the inlet flow parameters are all uniform. The inlet turbulence intensity is 10%. The "hub" is set as 'symmetry' condition. The 'casing' is set as a moving wall to simulate the relative motion between the blade tip and the casing, because it was found that effects of the centrifugal force and the Coriolis force were much smaller than the effect relative endwall motion (Yang et al. [25] and Acharya and Moreaux [26]). The flow coefficient is 0.4. The cascade exit Mach number is 1.2 and the exit Reynolds number (based on chord) is 1.7×10^6.

The blade surface heat transfer coefficient (*HTC*) is obtained based on the results of two calculations. One with blade surface set as adiabatic wall and the other with blade surface set as isothermal wall with wall temperature of T_w. *HTC* is defined as follows:

$$HTC = \frac{q}{T_{ad} - T_w} \qquad (1)$$

where q is the local heat flux obtained in the calculation with isothermal wall temperature of T_w, T_{ad} is the adiabatic wall temperature obtained in the calculation with adiabatic wall condition. In the current study, T_w is 197K, which gives an engine representative gas to wall temperature ratio of 1.5.

The mesh sensitivity study is conducted on the winglet tip 'PSW' at a tip clearance of 2.1%*C*. Three different mesh quantities of 6.5 million, 8.5 million and 10 million are used. The mesh was refined in the spanwise direction. The tip average y^+ and average heat transfer coefficient are listed in Table 2. The tip average *HTC* decreases by 1.8% and 1.9% when the mesh quantity increases from 6.5 million to 8.4 million and 10 million.

	Mesh-1	Mesh-2	Mesh-3
Mesh quantity (million)	6.5	8.4	10
Tip average y^+	2.1	1.3	1.2
Tip average HTC($W/m^2\cdot K$)	1213.1	1191.7	1189.7

Table 2 Mesh sensitivity study of winglet tip 'PSW' at tip clearance of 2.1%*C*

Experimental Validation

Fig. 3 shows the experimental and predicted tip *HTC* of the winglet tip 'PSW' without endwall motion at two tip clearances of 1.1%*C* and 2.1%*C* for validation. The details of the experiment and the result analysis for tip clearance of 2.1%*C* have been reported in [18]. The *HTC* is obtained by the same method used by Ma et al. [27]. The experimental uncertainty of the tip area-weighted averaged *HTC* is ±9.4%. The *HTC* is quite high on the pressure side winglet surface. As the tip clearance increases, the *HTC* on the cavity floor surface and on the suction side winglet surface increases, while the *HTC* on the pressure side winglet surface decreases. The CFD well predicts these trends.

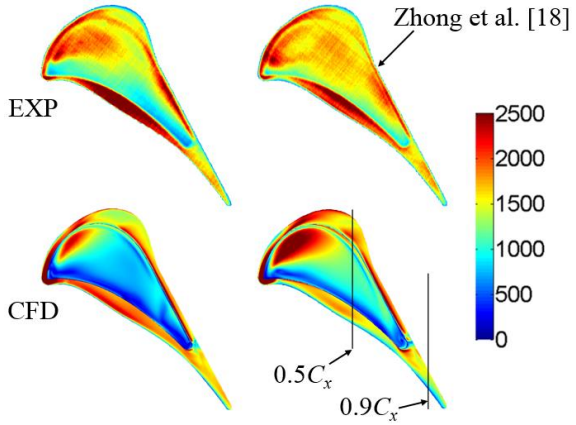

(a) $\tau = 1.1\%C$ (b) $\tau = 2.1\%C$

Fig. 3 Experimental and predicted tip heat transfer coefficient of winglet tip 'PSW' without endwall motion

Fig. 4 presents the *HTC* distribution at two axial locations of $0.5C_x$ and $0.9C_x$ as indicated in Fig. 3b. In Fig. 4a, both the CFD and experiment show that the *HTC* is relatively low inside the cavity. The CFD under predicts the *HTC* value on the pressure side winglet and inside the cavity, but agrees well with the experiment on the suction side winglet. In Fig. 4b, the CFD result shows that *HTC* decreases as tip clearance increases. However, the experimental result shows that the *HTC* decreases on the pressure side but increases on the suction side. Note that at the two locations, the discrepancy is large near the blade tip edge and squealer corner. One possible reason is that the blade tip edge radius is not considered in the calculation, so the flow separation above the squealer/winglet can not be modelled accurately. Another reason is that the 3-dimentional conduction effect is ignored in the experimental data processing.

Fig. 5 shows the relative *HTC* difference between the numerical and experimental results. Inside the cavity, the CFD

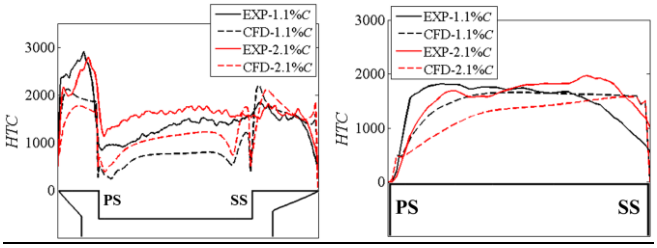

(a) (b)

Fig. 4 Comparison of heat transfer coefficient at two axial locations of (a) $0.5C_x$ and (b) $0.9C_x$

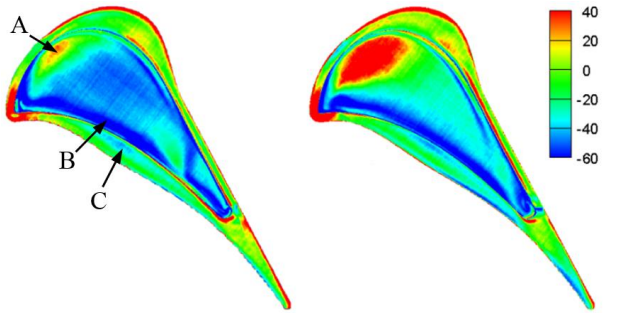

(a) $\tau = 1.1\%C$ (b) $\tau = 2.1\%C$

Fig. 5 Relative difference of tip heat transfer coefficient of winglet tip 'PSW' without endwall motion (percent)

under predicts the *HTC* in most areas except for region 'A'. The biggest difference occurs in region 'B' near the pressure side winglet, where the CFD under predicts the *HTC* by 50% to 75%. On the pressure side, suction side winglet surfaces and near the trailing edge region, the relative difference is mainly within ±20% except for region 'C' and the blade tip edge.

RESULTS AND DISCUSSION

The results presented in this part are obtained by numerical methods with relative endwall motion. Besides, all the flow field results are obtained based on the simulations with the 'blade' and 'casing' set as the adiabatic wall.

Tip Heat Transfer Results

Fig. 6 shows the distribution of tip heat transfer coefficient of different tip geometries with endwall motion. For the cavity tip, as the tip clearance increases, the *HTC* on the cavity floor surface generally increases. The area of high *HTC* region 'A' and 'C' becomes bigger while the area of low *HTC* region 'B' becomes smaller. The *HTC* above the pressure side squealer decreases with the tip clearance.

Compared with the cavity tip, the suction side winglet has little effect on the *HTC* distribution above the pressure side squealer and on the cavity floor surface at all tip clearances. The pressure side winglet slightly reduces the *HTC* on the cavity floor, but the distribution pattern is very similar with that of the cavity tip. The *HTC* on the pressure side winglet is much higher than that on the suction side winglet. As the size of the tip gap increases from 1.1%*C* to 3.1%*C*, the *HTC* on the pressure side winglet first increases and then decreases. The winglets mainly change the flow structure locally above the winglet geometries, and the *HTC* distribution on the suction side winglet of 'SSW' and 'PSW' is very similar. So, the tip flow structure of winglet tip 'PSW' will be presented to explain the tip heat transfer results.

Fig. 7 shows the *HTC* distribution on inner vertical squealer surface of winglet tip 'PSW'. The results of cavity tip and winglet tip 'SSW' are not presented because they are quite similar with the result of 'PSW'. At the smallest tip clearance, the *HTC* is less than 1000W/m^2·K in most areas. A local high-*HTC* spot appears in region 'A' on the pressure side and the maximum *HTC* value is about 2900W/m^2·K. As the tip clearance increases, the *HTC* increases because the flow velocity inside the cavity near the vertical squealer increases with the tip clearance as shown in Fig. 10 and Fig. 11. At tip clearances of 2.1%*C* and 3.1%*C*, the *HTC* in region 'B' and 'C' is relatively larger. The maximum value in region 'B' is

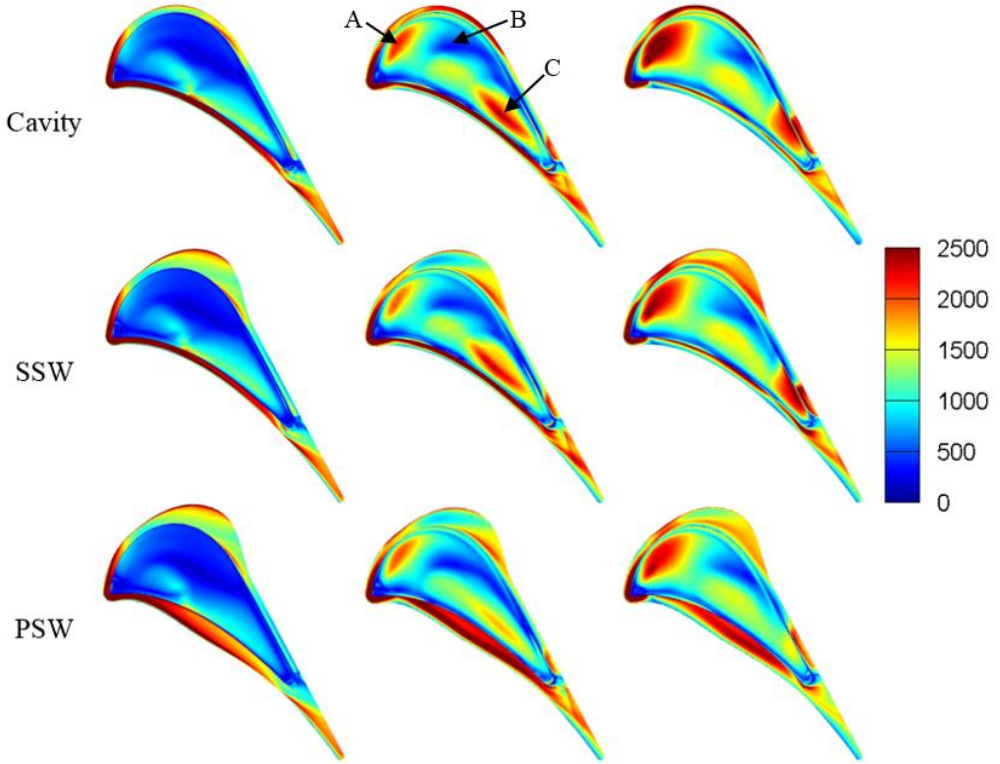

(a) τ = 1.1%C (b) τ = 2.1%C (c) τ = 3.1%C

Fig. 6 Tip *HTC* distribution of all tips

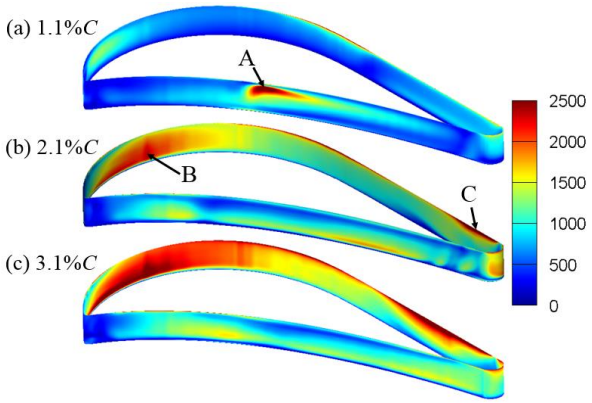

Fig. 7 *HTC* distribution on inner vertical squealer surface of winglet tip 'PSW'

2300W/m^2·K and 2900W/m^2·K for τ = 2.1%C and τ = 3.1%C respectively, while it is about 4600W/m^2·K in region 'C' for the two tip clearances.

Fig. 8 shows the Mach number distributions and two-dimensional streamlines on the cut plane in the middle of the tip gaps of winglet tip 'PSW'. The dark contour lines correspond to Ma = 1. The flow enters the tip gap from the pressure side and front part of the suction side region. At all tip clearances, the subsonic flow dominates the region inside the tip gap except for the region above the suction side squealer after the middle chord, where the flow becomes supersonic. The flow inside the tip gap is deflected due to the shear force caused by the endwall motion. The flow is deflected more towards the tangential direction at a smaller tip gap. The Mach number of the flow within the tip cavity generally increases with the tip clearance.

Fig. 9 shows the 3D tip flow streamlines of winglet tip

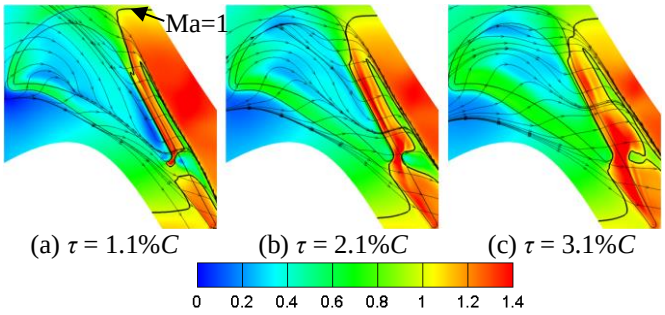

(a) τ = 1.1%C (b) τ = 2.1%C (c) τ = 3.1%C

Fig. 8 Mach number on the middle plane of the tip gap of winglet tip 'PSW'

'PSW' coloured by flow Mach number at three tip clearances. Near the leading edge, the flow enters the tip gap and impinges on the cavity floor surface, which results in the high *HTC* region 'A' shown in Fig. 6b. Then the flow rolls up to form the 'Leading Edge Vortex'(LEV). Above the pressure side winglet, the flow first separates and then reattaches on the winglet surface, which results in local high *HTC* as shown in Fig. 6. The height and length of the separation zone increases as the tip clearance increases. Inside the cavity, the flow entering from the pressure side rolls up to form the 'Cavity Vortex'(CV), the size of which increases as the tip clearance increases. It is interesting to find that at the smallest tip clearance, the cavity vortex seems to be divided into two parts: the part near leading edge has a relatively larger size while the other is smaller and is confined to the pressure side squealer corner. It is the impingement of the cavity vortex that leads to the high *HTC* region 'B' shown in Fig. 6b. The flow near the casing is strongly affected by the endwall motion and it rolls up to form the 'Cavity Scraping Vortex'(CSV). On the contrary to the 'Cavity Vortex', the size of this vortex reduces

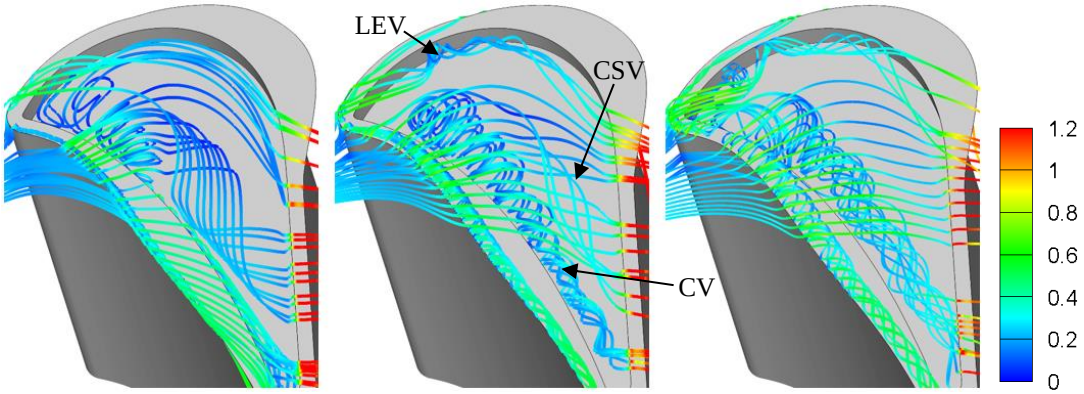

(a) τ = 1.1%C (b) τ = 2.1%C (c) τ = 3.1%C

Fig. 9 Tip flow streamlines of winglet tip 'PSW'

as the tip clearance increases, which will be further discussed later.

Fig. 10 shows the Mach number contours along with two-dimensional streamlines on a cross section plane in the frontal blade passage of winglet tip 'PSW'. As the tip clearance increases, the size of both the separation bubble above the pressure side winglet and suction side winglet becomes larger. Note that the flow hardly reattaches on the top of the pressure side winglet at the largest tip clearance. Above the cavity floor, the structures of the cavity vortex, the cavity scraping vortex and the leading edge vortex can be identified clearly. In Fig. 10a, 'P1' indicates the impingement singularity point, and 'P2' indicates the separation singularity point, at which the flow begins an upward motion and results in very low *HTC* in region 'B' shown in Fig. 6b.

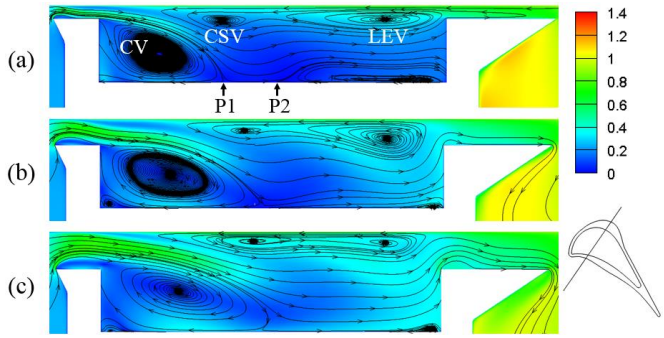

Fig. 10 Mach number distribution on the cross section plane in the blade frontal region of winglet tip 'PSW': (a) 1.1%C, (b) 2.1%C, and (c) 3.1%C

Fig. 11 shows the Mach number contours along with two-dimensional streamlines on a cross section plane in the rear blade passage of winglet tip 'PSW'. As tip clearance increases, the size of cavity vortex increases and the size of the cavity scraping vortex decreases. The cavity scraping vortex impinges on the cavity floor surface at tip clearance of 1.1%C and 2.1%C, causing high-*HTC* region 'C' in Fig. 6b. At the smallest tip clearance of 1.1%C, the size of the cavity vortex on this plane is much smaller than that shown in Fig. 10a, which is consistent with that observed in Fig. 9a.

Fig. 12 shows the wall shear stress and the limit streamline on the cavity floor surface of winglet tip 'PSW'. The distribution pattern of the wall shear stress is consistent

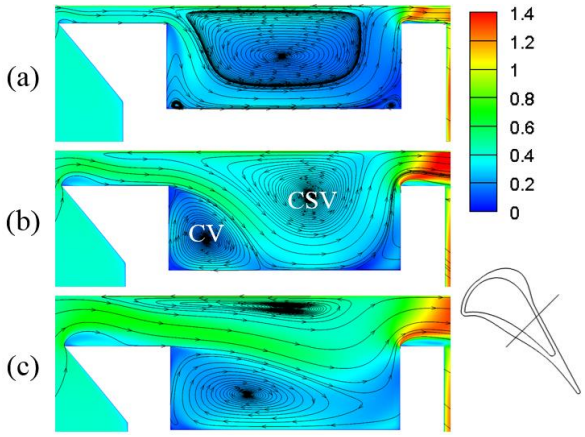

Fig. 11 Mach number on the cross section plane in the blade rear part region of winglet tip 'PSW': (a) 1.1%C, (b) 2.1%C, and (c) 3.1%C

with the *HTC* distribution pattern shown in Fig. 6. The red dashed line indicates the impingement singularity ('P1' in Fig. 10a) and the white dashed line indicates the separation singularity ('P2' in Fig. 10a). With a larger tip clearance, the wall shear stress near the blade leading edge is bigger, which reveals a stronger impingement effect in this region and hence higher *HTC*. At τ = 3.1%C, the high-*HTC* region 'C' shown in Fig. 6b is located below the red dashed line, which indicates that the high *HTC* here is mainly caused by the impingement of the cavity vortex. However, for tip clearance of 1.1%C and 2.1%C, part of the high *HTC* region 'C' is located above the red dashed line, indicating that cavity scraping vortex is partly responsible for the high *HTC* on the cavity floor. This has been proven by Fig. 11, which shows that the cavity scraping vortex is very close to the cavity floor surface and the impingement effect is significant at these two tip clearances. The white dashed line in the low wall shear stress region shows that the low *HTC* on the cavity floor is mainly caused by the flow upward motion induced by the cavity scraping vortex.

Fig. 13 shows the area-weighted average *HTC* on the blade tip of all tips. In general, the average *HTC* increases with the tip clearance. At the smallest tip clearance of 1.1%C, the difference between the average *HTC* of all tips is negligible. Compared with the cavity tip, the winglet tip 'SSW' reduces the average *HTC* by 2.2% and 1.7% for τ = 2.1%C and τ = 3.1%C respectively, and the corresponding decrement of

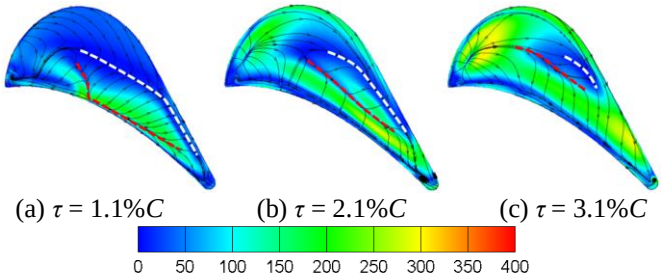

Fig. 12 Wall shear stress limit streamline on cavity floor surface of winglet tip 'PSW'

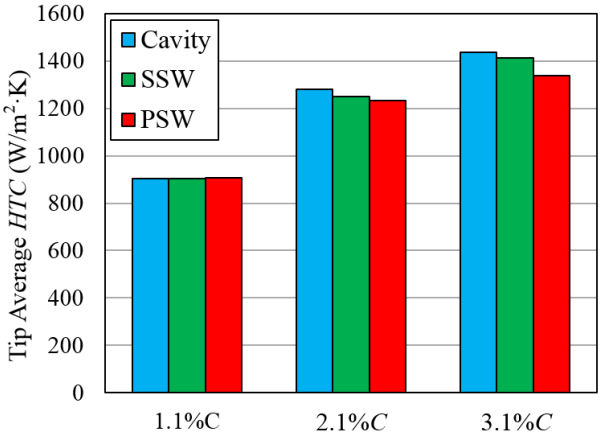

Fig. 13 Tip average *HTC* of all tips at three tip clearances

winglet tip 'PSW' is 3.7% and 6.7%.

The heat load Q is another important parameter for heat transfer study. It is defined as follows:

$$Q = \int_A q dA \qquad (2)$$

where q is the local heat flux in the small area dA. For a blade tip, a higher heat load requires a larger mass of the coolant flow, which may reduce the engine performance. Fig. 14 shows the total heat load on the tip surface at three tip clearances. The heat load is normalized by the total tip heat load of cavity tip at the smallest tip clearance of 1.1%C. For all tips, the total tip heat load increases with the tip clearance. The winglet tip 'PSW' has the largest heat load because it has the largest tip surface area. At the largest tip clearance, the heat load of winglet tip 'PSW' and 'SSW' is nearly the same.

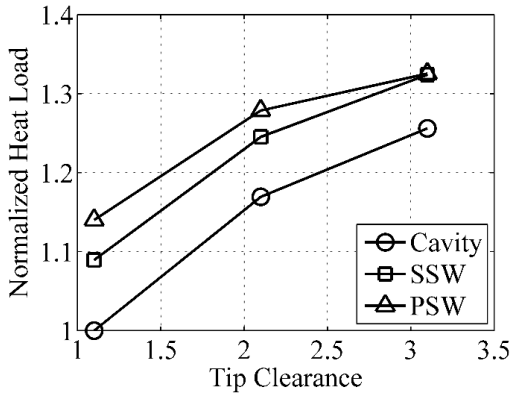

Fig. 14 Normalized total heat load on the tip surface

Blade Suction Side Heat Transfer Results

Fig. 15 shows the *HTC* distribution on the blade suction side surface for all tips at different tip clearances. A high-*HTC* strip (indicated by 'A' in Fig. 15a) appears near the tip region. Specifically, the *HTC* is quite high on the side surface of the suction side winglet (indicated by 'B' in Fig. 15a).

Fig. 16 shows the total pressure loss coefficient and velocity vector on the same plane as Fig. 10 of cavity tip and winglet tip 'SSW'. For both tips, after the tip leakage flow discharges from the tip gap, it interacts with the main flow and rolls up to form the tip leakage vortex. The flow deflects its direction and has an impingement effect on the side surface of the blade, which causes the high *HTC* in area 'B' shown in Fig. 15. There is little difference between the *HTC* distributions of the two winglet tips, as the pressure side winglet has little effect on the tip leakage vortex structure. The interesting thing is that the *HTC* in region 'A' generally increases with the tip clearance for the cavity tip, but it decreases with tip clearance for the two winglet tips. Why is this the case?

Fig. 17 shows the total pressure loss coefficient on a cut plane normal to blade suction side edge of cavity tip and winglet tip 'SSW'. For both tips, the size of tip leakage vortex increases as the tip clearance increases. For the cavity tip, the tip leakage vortex attaches on the blade surface and the distance between the vortex core and the blade wall changes little at all tip clearances. So the *HTC* on the blade wall increases mainly because more fluid impinges on the wall at a larger tip clearance. However, for winglet tip 'SSW', the tip leakage vortex becomes further away from the blade wall as the tip clearance increases, which reduces the impingement

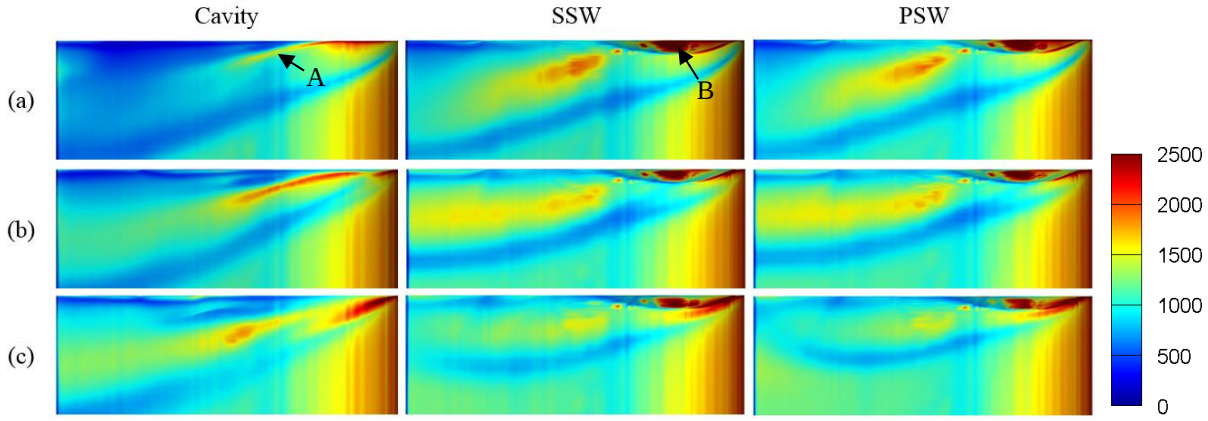

Fig. 15 *HTC* distribution on blade suction side surface: (a) 1.1%C, (b) 2.1%C, and (c) 3.1%C

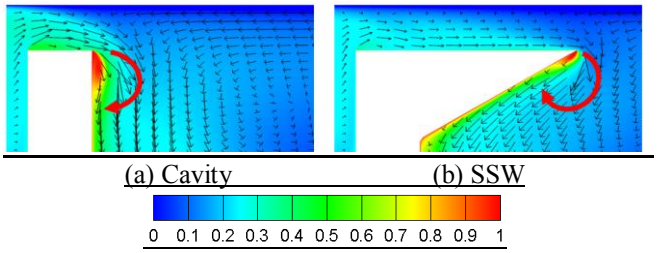

Fig. 16 Total pressure loss coefficient and velocity vector on the same plane as shown in Fig. 10 of cavity tip and winglet tip 'SSW'

effect of the vortex. This is why the *HTC* on the blade wall decreases with the tip clearance. In addition, it is very interesting to find that the total pressure loss coefficient in the tip leakage vortex region is reduced by such a small suction side winglet, and the passage vortex is also suppressed at all tip clearances.

Fig. 18 shows the area-weighted average *HTC* on the blade suction side surface of all tips. The average *HTC* of the cavity tip increases with the tip clearance and is the lowest at all tip clearances. There is little difference between the two winglet tips, indicating that the pressure side winglet has little effect on the tip leakage vortex structure in this study. Compared with the cavity tip, the two winglets increase the average *HTC* by 5.0%, 2.7% and 0.9% at tip clearance of 1.1% *C*, 2.1%*C* and 3.1%*C* respectively.

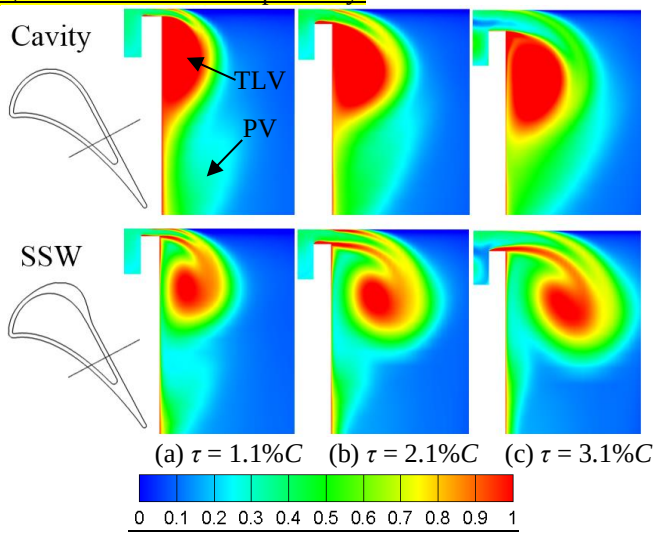

Fig. 17 Total pressure loss coefficient on a cut plane normal to blade suction side of cavity tip and winglet tip 'SSW'

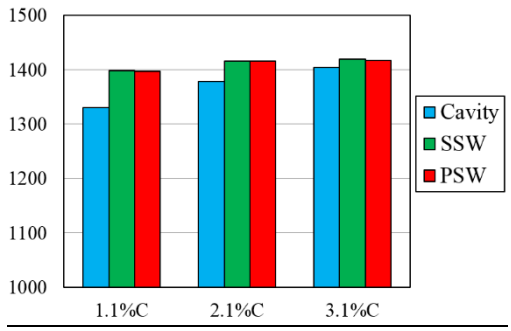

Fig. 18 Average *HTC* on blade suction side surface of all tips at three tip clearances

CONCLUSIONS

This paper investigates the thermal performance of two cavity-winglet tips with endwall motion under transonic conditions at three tip clearances of 1.1%, 2.1% and 3.1% chord. The conclusions can be drawn as follows:

1. The effects of tip gap size on the thermal performance of cavity-winglet tips are significant. The average tip *HTC* and total tip heat load increase as the size of the tip gap increases.
2. The *HTC* on inner vertical squealer surface generally increases with the tip clearance because the flow velocity inside the cavity near the vertical squealer increases with the tip clearance.
3. With a pressure side winglet, the tip leakage flow reattaches on the top surface of the winglet after the separation from the pressure side edge, which results in high *HTC*. The size of the separation bubble over the pressure side winglet increases with the tip clearance.
4. Inside the cavity, as the tip clearance increases, the size of the cavity vortex increases, resulting in higher heat transfer. The cavity scraping vortex becomes smaller and lifts off from the cavity floor surface, which reduces the area of the low *HTC* region on the cavity floor. The cavity scraping vortex also increases the *HTC* on the cavity floor at tip clearance of 1.1%*C* and 2.1%*C* because it is very close to the floor surface and its impingement effect is evident.
5. The *HTC* in the near-tip region on the blade suction side wall of the two winglet tips decreases with the tip clearance, showing opposite trend to that of the cavity tip. This is because the tip leakage vortex of the two winglet tips locates further away from the blade wall as the tip clearance increases, reducing the impingement effect of the tip leakage vortex.
6. The *HTC* is high on the side surface of the suction side winglet at all tip clearances because of the tip leakage flow impingement.

NOMENCLATURE

C	Blade chord
C_x	Axial chord
H	Blade span (used in the computation)
s	Local curve length of the suction side
S	Total curve length of the suction side
τ	Tip gap size
t	Pitch
C_{p0}	Total pressure loss coefficient = $(P_{01}-P_0)/(P_{01}-P_2)$
HTC	Heat transfer coefficient = q / $(T_{ad} - T_w)$
Ma	Mach number
Re	Reynolds number = $\rho VC/\mu$
P_0	Total pressure
T_0	Total temperature
T_{ad}	Adiabatic wall temperature
T_w	Wall temperature
q	Local heat flux
V	Velocity
ρ	Density
μ	Dynamic viscosity
φ	Flow coefficient

Subscripts

1 Cascade inlet
2 Cascade exit

ACKNOWLEDGMENTS

The authors would like to acknowledge the support of the National Natural Science Foundation of China (NSFC), Grant No.51576003.

REFERENCES

[1] Denton JD, "Loss mechanisms in turbomachines", ASME Paper No. 93-GT-435, 1993

[2] Heyes FJG, Hodson HP, and Dailey GM, "The effect of blade tip geometry on the tip leakage flow in axial turbine cascades", ASME J. Turbomach., 114(3), 1992, pp 643-651

[3] Key NL, and Arts T, "Comparison of turbine tip leakage flow for flat tip and squealer tip geometries at high speed conditions", ASME J. Turbomach., 128(2), 2006, pp 213-220

[4] Lee SW, and Kim SU, "Tip gap height effects on the aerodynamic performance of a cavity squealer tip in a turbine cascade in comparison with plane tip results: part 1 – tip gap flow structure", Exp. Fluids, 49(5), 2010, pp 1039-1051

[5] Schabowski Z, Hodson H, Giacche D, Power B, and Stokes MR, "Aeromechanical optimization of a winglet-squealer tip for an axial turbine", ASME J. Turbomach., 136(7), 2014, p 071004

[6] Zhou C, Hodson H, Tibbott I, and Stokes M, "Effects of winglet geometry on the aerodynamic performance of tip leakage flow in a turbine cascade", ASME J. Turbomach., 135(5), 2013, p 051009

[7] Cheon JH, and Lee SW, "Tip leakage aerodynamics over the cavity squealer tip equipped with full coverage winglets in a turbine cascade", Int. J. Heat Fluid Flow, 56, 2015, pp 60-70

[8] Harvey N, Newman D, and Haselbach F, "An investigation into a novel turbine rotor winglet. part 1: design and model rig test results", ASME Paper No. GT2006-90456, 2006

[9] Bunker RS, "A review of turbine blade tip heat transfer in gas turbine systems", Ann. N.Y. Acad. Sci., 934, 2001, pp 64-79

[10] Teng S, Han JC, and Azad GMS, "Detailed heat transfer coefficient distributions on a large-scale gas turbine blade tip", Journal of Heat Transfer, 123(4), 2001, pp 803-809

[11] Bunker RS, and Bailey JC, "Effect of squealer cavity depth and oxidation on turbine blade tip heat transfer", ASME Paper No. 2001-GT-0155, 2001

[12] Kwak JS, and Han JC, "Heat transfer coefficients on the squealer tip and near squealer tip regions of a gas turbine blade", ASME J. Heat Transfer, 125, 2003, pp 669-677

[13] Azad GS, Han J, and Boyle RJ, "Heat transfer and flow on the squealer tip of a gas turbine blade", ASME J. Turbomach., 122(4), 2000, pp 725-732

[14] Newton PJ, Krishnababu SK, Lock GD, Hodson HP, Dawes WN, Hannis J, and Whitney C, "Heat transfer and aerodynamics of turbine blade tips in a linear cascade", ASME J. Turbomach., 128(2), 2006, pp 300-309

[15] Papa M, Goldstein RJ, and Gori F, "Effects of tip geometry and tip clearance on the mass/heat transfer from a large-scale gas turbine blade", ASME J. Turbomach., 125, 2003, pp 90-96

[16] Saha AK, Acharya S, Prakash C, and Bunker RS, "Blade tip leakage flow and heat transfer with pressure side winglet", International Journal of Rotating Machinery, 1, 2006, pp 1-15

[17] O'Dowd DO, Zhang Q, He L, Oldfield MLG, Ligrani PM, Cheong BCY, and I Tibbott, "Aero-thermal performance of a winglet at engine representative Mach and Reynolds numbers", ASME Paper No. GT2010-22794, 2010

[18] Zhong F, Zhou C, Ma H, and Zhang Q, "Heat transfer of winglet tips in a transonic turbine cascade", ASME Paper No. GT2016-56804, 2016

[19] Tallman J, and Lakshminarayana B, "Numerical simulation of tip leakage flows in axial flow turbines, with emphasis on flow physics: part II – effect of outer casing relative motion", ASME J. Turbomach., 123(2), 2001, pp 324-333

[20] Yaras MI, and Sjolander SA, "Effects of simulated rotation on tip leakage in a planar cascade of turbine blades: part I – tip gap flow", ASME J. Turbomach., 114(3), 1992, pp 652-659

[21] Palafox P, Oldfield MLG, Ireland PT, Jones TV, and LaGraff JE, "Blade tip heat transfer and aerodynamics in a large scale turbine cascade with moving endwall", ASME J. Turbomach., 134(2), 2012, p 21020

[22] Zhou C, "Effects of endwall motion on thermal performance of cavity tips with different squealer width and height", International Journal of Heat and Mass Transfer, 91, 2015, pp 1248-1258

[23] Rhee DH, and Cho HH, "Local heat/mass transfer characteristics on a rotating blade with flat tip in a low-speed annular cascade – part 2: tip and shroud", ASME J. Turbomach., 128, 2006, pp 110-119

[24] Zhou C, and Zhong F, "A Novel Suction Side Winglet Design Method for High Pressure Turbine Rotor Tips", ASME Paper No. GT2016-56218, 2016

[25] Yang D, Yu X, and Feng Z, "Investigation of leakage flow and heat transfer in a gas turbine blade tip with emphasis on the effect of rotation", ASME J. Turbomach., 132(4), 2010, p 041010

[26] Acharya S, and Moreaux L, "Numerical study of the flow past a turbine blade tip: effect of relative motion between blade and shroud", ASME J. Turbomach., 136(3), 2013, p 031015

[27] Ma H, Wang Z, Wang L, Zhang Q, Yang Z, Bao Y, "Ramp Heating in High-Speed Transient Thermal Measurement with Reduced Uncertainty", ASME Paper No. GT2015-43012

Comments and reply

PAPER: 60

TITLE: Tip Gap Size Effects on Thermal Performance of Cavity-winglet Tips in Transonic Turbine Cascade with Endwall Motion

AUTHORS: Chao Zhou and Fangpan Zhong

REVIEW 1

---------- Minor Revisions ----------

1. Conclusion #6

Please add some comments in the manuscript to prove that high HTC on the side surface of the suction side winglet is due to the tip leakage flow impingement.

Re: Thank you for your suggestion. Fig. 16 has been added in the revised paper to prove that high HTC on the side surface of the suction side winglet is due to the tip leakage flow impingement. The related discussion is added on Page 6 as follows:

"Fig. 16 shows the total pressure loss coefficient and velocity vector on the same plane as Fig. 10 of cavity tip and winglet tip 'SSW'. For both tips, after the tip leakage flow discharges from the tip gap, it interacts with the main flow and rolls up to form the tip leakage vortex. The flow deflects its direction and has an impingement effect on the side surface of the blade, which causes the high HTC in area 'B' shown in Fig. 15."

2. First sentence of the second paragraph on page 5

"it is the impingement of the cavity vortex mainly results in the high HTC." needs to be corrected.

Re: Thank you for your suggestion. This sentence has been corrected as "……which indicates that the high *HTC* here is mainly caused by the impingement of the cavity vortex."

3. Last sentence of the fourth paragraph on page 5

Please correct the sentence of "At the largest tip clearance, the heat load of winglet tip 'PSW' and 'SSW' is the nearly the same.".

Re: Thank you for pointing out this mistake. This sentence has been corrected as "At the largest tip clearance, the heat load of winglet tip 'PSW' and 'SSW' is nearly the same." This sentence is now on Page 6.

4. The results for 2.1%C seem to be published by Zhong et al. (2016). "[18]" needs to be added in the figures that have the 2.1%C data.

Re: Thank you for your suggestion. Fig. 3 has been updated by adding the "Zhong et al. [18]" into the figure.

REVIEW 2

---------- Major Revisions ----------

1. Report the design principles behind the chosen winglet geometries. Were the original design objectives matched in practice (CFD and experiments)?

Re: Thank you for your comment. It is now stated on Page 2 in the revised paper that "The design of the suction side winglet is based on the method proposed by Zhou and Zhong [19]."
([19] Zhou C, and Zhong F, "A Novel Suction Side Winglet Design Method for High Pressure Turbine Rotor Tips", ASME Paper No. GT2016-56218, 2016)

Fig. 19 shows the tip leakage loss coefficient of the three tips at different tip clearance. The two winglet tips outperform the cavity tip at tip clearances of 2.1%*C* and 3.1%*C*. But the tip leakage loss is almost the same at the smallest tip clearance of 1.1%*C*. Since this paper mainly focuses on the thermal performance of the three blade tips, this figure is not presented in the revised paper.

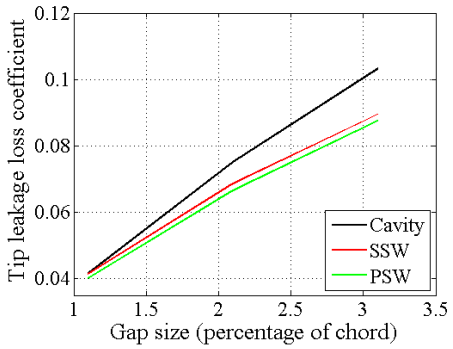

Fig. 19 Tip leakage loss coefficient of the three tips at different tip clearance

2. The CFD method requires a more detailed analysis and a quantitative assessment of the grid independency. While the authors report variations in tip heat transfer with the mesh density, it is not clear if the mesh of 10Million has reached convergence. I would recommend the use of standard grid independency methods to carry out this study and I would add details on how and where the mesh was refined.

Re: Thank you for your comment. More details about the grid independency is added on Page 2 in the revised paper as follow:

"The mesh was refined in the spanwise direction. The tip average y^+ and average heat transfer coefficient are listed in Table 4. The tip average HTC decreases by 1.8% and 1.9% when the mesh quantity increases from 6.5 million to 8.4 million and 10 million."

	Mesh-1	Mesh-2	Mesh-3
Mesh quantity (million)	6.5	8.4	10
Tip average y^+	2.1	1.3	1.2
Tip average HTC($W/m^2 \cdot K$)	1213.1	1191.7	1189.7

Table 4 Mesh sensitivity study of winglet tip 'PSW' at tip clearance of 2.1%*C*

3. The comparison CFD-EXP must be improved:

a. Report detailed comparison between CFD and EXP at distinct axial locations. It is difficult for the reader to assess the discrepancy between the contour plots. Report also a contour plot with relative difference between EXP and CFD (to quantify the differences).

Re: Thank you for your suggestions. The detailed comparison between CFD and EXP at two axial locations of $0.5C_x$ and $0.9C_x$ have been added in Fig. 4 in the revised paper. And the related discussion has been added on Page 3 as follows:

"Fig. 4 presents the HTC distribution at two axial locations of 0.5Cx and 0.9Cx as indicated in Fig. 3b. In Fig. 4a, both the CFD and experiment show that the HTC is relatively low inside the cavity. The CFD under predicts the HTC value on the pressure side winglet and inside the cavity, but agrees well with the experiment on the suction side winglet. In Fig. 4b, the CFD result shows that HTC decreases as tip clearance increases. However, the experimental result shows that the HTC decreases on the pressure side but increases on the suction side. Note that at the two locations, the discrepancy is large near the blade tip edge and squealer corner. One possible reason is that the blade tip edge radius is not considered in the calculation, so the flow separation above the squealer/winglet can not be modelled accurately. Another reason is that the 3-dimentional conduction effect is ignored in the experimental data processing."

The contour plots of relative difference between EXP and CFD have been added in Fig. 5 in the revised paper. The related discussion has also been added on Page 3 as follows:

"Fig. 5 shows the relative HTC difference between the numerical and experimental results. Inside the cavity, the CFD under predicts the HTC in most areas except for region 'A'. The biggest difference occurs in region 'B' near the pressure side winglet, where the CFD under predicts the HTC by 50% to 75%. On the pressure side, suction side winglet surfaces and near the trailing edge region, the relative difference is mainly within ±20% except for region 'C' and the blade tip edge."

b. Focus the detail of the comparison on the blade tip rims/winglets. It is at these locations that the prediction of the heat transfer is crucial.

Re: Thank you for your suggestion. The detail of the comparison on the blade tip winglets have been added in Fig. 4 and Fig. 5 and the related discussions are added on Page 3 in the revised paper as mentioned above.

c. Report experimental uncertainty.

Re: Thank you for your suggestion. The experimental uncertainty has been reported on Page 3 in the revised paper as follows:
"The experimental uncertainty of the tip area-weighted averaged HTC is ±9.4%."

d. Report the methodology used in the experiments to calculate the heat transfer shown in Figure 3. Comment on possible discrepancy and errors arising from the use of non-conjugate approach where solid conduction is not solved (both CFD and EXP).

Re: Thank you for your suggestion. The methodology used in the experiment to calculate the heat transfer coefficient has been added in the revised paper on Page 3 as follows:

"The heat transfer coefficient is obtained by the same method used by Ma et al. [27]."

([27] Ma H, Wang Z, Wang L, Zhang Q, Yang Z, Bao Y, "Ramp Heating in High-Speed Transient Thermal Measurement with Reduced Uncertainty", ASME Paper No. GT2015-43012

The one-dimensional semi-infinite assumption is adopted in the experimental data processing to obtain the heat transfer coefficient, so the experimental error could be significant for the blade trailing edge, the blade tip corner and the squealer/winglet surface, where the 3D heat conduction effect is important. This has been pointed out on Page 3 in the revised paper.

The CFD uses the non-conjugate approach to obtain the HTC. The authors think that this mainly affects the local HTC value, but not the general HTC distribution pattern.

e. In order to evaluate the performance of the numerical method, it will be ideal to compare the CFD rotor losses with the experimental values.

Re: Thank you for your suggestion. We also want to compare the aerodynamic performance, but there are no experimental rotor loss results for our current study.

f. The authors have used uniform inlet profiles for their CFD calculations (what about the experiments?). It will be extremely useful to verify that real-engine non-uniform profiles (flow field at the stator outlet), have not a significant influence on the absolute and relative performance of the 3 tip geometries. Does the CFD inlet profiles match the experimental ones?

Re: The authors did not measure the inlet boundary layer profile due to the limit of test instrument. However, the authors did an CFD study on the effect of inlet locations on the blade heat transfer based on the cavity tip at tip clearance of 2.1% chord. Three inlet locations (0.3Cx, 1Cx and 2Cx before the blade leading edge) are used to model different inlet conditions, e.g. inlet boundary layer velocity profile. Fig. 20 shows the total pressure profile and velocity profile for different inlet locations at $0.3C_x$ before blade leading edge. The vertical coordinate is the ratio of distance from casing wall to the tip gap size. Fig. 21 shows three tip heat transfer coefficient (HTC) distributions and Fig. 22 shows the pitch-wise average HTC distributions along the axial direction. The two figures show that the difference between them is very small. Table 3 presents the tip area-weighted average HTC of the three cases and the variations are also very small.

As for HTC on blade suction surface, Fig. 23 shows its distributions and Fig. 24 shows spanwise average HTC distributions around the blade suction surface. As inlet location goes further from blade leading edge, the high-HTC on the blade suction surface gets larger. Zhang et al. [1] attribute this to the interaction and balance between the passage vortex and the tip leakage flow. A good news is that the distribution patterns on the blade suction surface are very similar for the three cases.

[1] Q. Zhang, L. He, A. Rawlinson, 2014, "Effects of Inlet Turbulence and End-Wall Boundary Layer on Aerothermal Performance of a Transonic Turbine Blade Tip," Journal of Engineering for Gas Turbines and Power, Vol. 136(5), pp. 1-7.

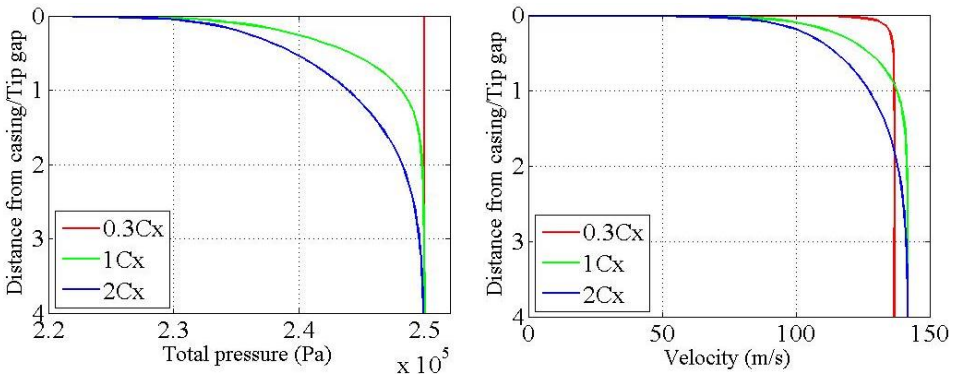

(a) Total pressure profile (b) Velocity profile

Fig. 20 Total pressure and velocity profiles for different inlet locations at 0.3C_x before blade leading edge

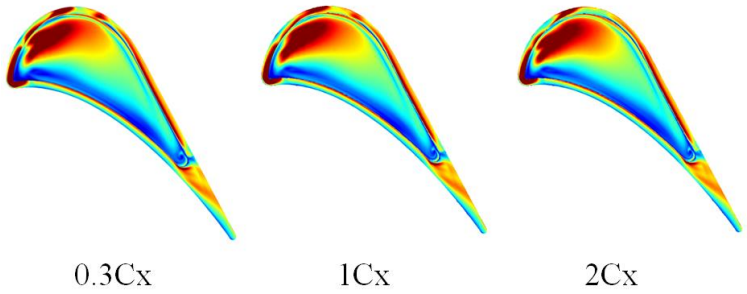

Fig. 21 Tip HTC distributions for different inlet locations

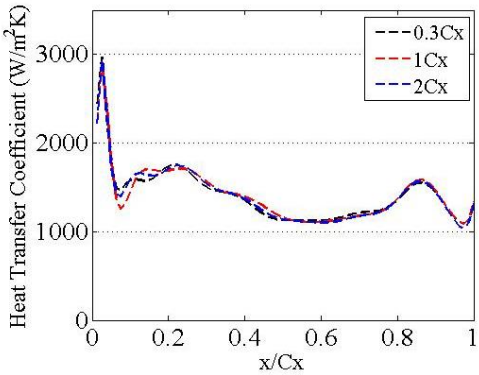

Fig. 22 Pitchwise average HTC distributions for different inlet locations

0.3Cx	1Cx	2Cx
1390.4	1393.8	1384.9

Table 3 Area-weighted averaged HTC on tip top surfaces for different inlet locations

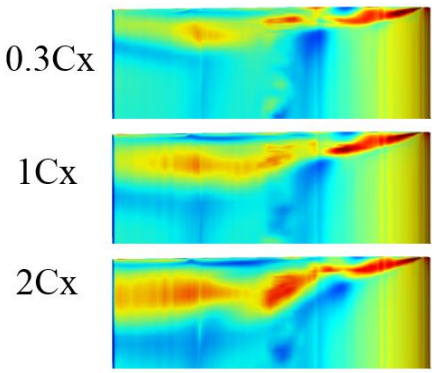

Fig. 23 HTC distributions on blade suction surface for different inlet locations

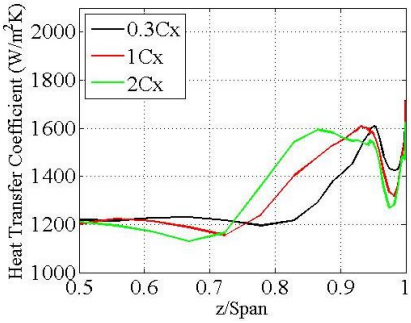

Fig. 24 Spanwise average HTC distributions around the blade suction surface for different inlet locations

4. The authors performed an adiabatic simulation to obtain the adiabatic wall temperature.

a. However, it is not clear what CFD simulation they used to analyze the blade tip cavity flow field (for example figures 6-7-8), the isothermal at Tw = 197 K or the adiabatic one?

Re: Thank you for your comment. It is now stated on Page 3 in the revised paper as follows: "Besides, all the flow field results are obtained based on the simulations with the 'blade' and 'casing' set as the adiabatic wall."

b. Have the authors checked the differences in adiabatic HTC calculated with 2 isothermal calculations (at Twall only few Kelvin apart), rather than 1 isothermal and one adiabatic?

Re: Thank you for your suggestion. Fig. 25 presents blade tip HTC distribution of winglet tip 'PSW' at tip clearance of 2.1%*C* by two different methods. Fig. 25a is the result in the current study obtained by setting one isothermal wall(197K) and one adiabatic wall. Fig. 25b is the result obtained by setting two isothermal walls(197K and 207K). Obviously, the HTC distribution patterns by these two methods are very similar. However, the HTC in Fig. 25b is generally larger than that in Fig. 25a . Fig. 17 shows the relative HTC difference(relative to the result in Fig. 25a) on blade tip surface. The relative difference is bigger on the suction side winglet surface than that on the pressure side winglet surface.

The aim of the current study is to understand the effect of tip clearance on the thermal performance of different winglet tips with endwall motion from the aspect of physical mechanism. The discrepancy caused by calculation method of HTC will not change the main conclusions in this paper.

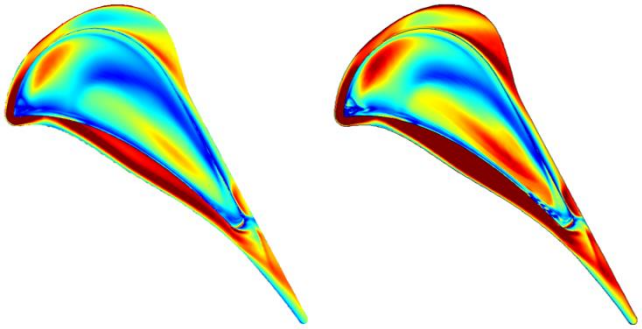

(a) Isothermal wall + Adiabatic wall (b) 2 Isothermal walls (10K apart)

Fig. 25 Tip HTC distribution of winglet tip 'PSW' at τ = 2.1%*C*

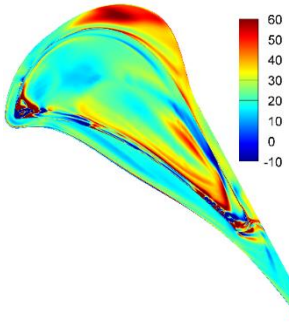

Fig. 26 Relative HTC difference on blade tip surface of winglet tip 'PSW' at τ = 2.1%*C*

5. The paper lacks more description and analysis of the winglet surface / inner vertical rim heat transfer (distributions, absolute levels) and of the aerodynamic sealing mechanisms offered by the winglet designs and the squealer ones. This information will be the most valuable to designers to select a specific winglet design and realize coolable winglet rotors.

Re: Thank you for your comment. The heat transfer result of inner vertical rim has been added in Fig. 7 and its description is added on Page 3 in the revised paper as follows:

"Fig. 7 shows the HTC distribution on inner vertical squealer surface of winglet tip 'PSW'. The results of cavity tip and winglet tip 'SSW' are not presented because they are quite similar with the result of 'PSW'. At the smallest tip clearance, the HTC is less than 1000W/m2·K in most areas. A local high-HTC spot appears in region 'A' on the pressure side and the maximum HTC value is about 2900W/m2·K. As the tip clearance increases, the HTC increases because the flow velocity inside the cavity near the vertical squealer increases with the tip clearance as shown in Fig. 10 and Fig. 11. At tip clearances of 2.1%C and 3.1%C, the HTC in region 'B' and 'C' is relatively larger. The maximum value in region 'B' is 2300W/m2·K and 2900W/m2·K for τ = 2.1%C and τ = 3.1%C respectively, while it is about 4600W/m2·K in region 'C' for the two tip clearances."

This paper focuses on the thermal performance of the winglet tips. We have another paper describing the design of winglet tip in a transonic turbine and also the aerodynamic sealing mechanism. (Zhou, C.*, and Zhong, F., "A Novel Suction Side Winglet Design Method for High Pressure Turbine Rotor Tips," 2016, ASME paper GT2016-56218.)

6. Can the author produce the same plot as in figure 10 for the blade suction side heat transfer?

Re: Thank you for your suggestion. The average HTC on blade suction side surface has been added in Figure 18 in the revised paper and the corresponding discussion is added on Page 7 as follows:

"Fig. 18 shows the area-weighted average HTC on the blade suction side surface of all tips. The average HTC of the cavity tip increases with the tip clearance and is the lowest at all tip clearances. There is little difference between the two winglet tips, indicating that the pressure side winglet has little effect on the tip leakage vortex structure in this study. Compared with the cavity tip, the two winglets increase the average HTC by 5.0%, 2.7% and 0.9% at tip clearance of 1.1% C, 2.1%C and 3.1%C respectively."

7. It will be interesting to quantify the aerodynamic performance of the 3 tip geometries at the rotor outlet rather than at one mid-chord axial plane only (Figure 13). Do the winglets actually outperform the squealer tip? At all tip clearances?

Re: Thank you for your suggestion. Fig. 17 shows the tip leakage loss coefficient of the three tips at different tip clearance. The two winglet tips outperform the cavity tip at tip clearances of 2.1%*C* and 3.1%*C*. But the tip leakage loss is almost the same at the smallest tip clearance of 1.1%*C* for the three tips. Since this paper mainly focuses on the thermal performance of the three blade tips, this figure is not presented in the revised paper.

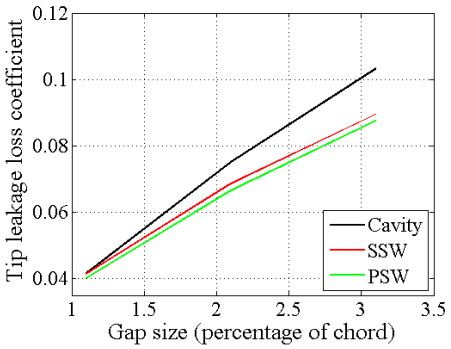

Fig. 27 Tip leakage loss coefficient of the three tips at different tip clearance

REVIEW 3

---------- Minor Revisions ----------

Suggest look into more details near the trailing edge region. Some conclusions about heat transfer trend might need rewording.

Re: Thank you for your suggestion. More details near the trailing edge region have been added in the 'Experimental Validation' part on Page 3. Conclusion 2 has been changed as follows:

"The HTC on inner vertical squealer surface generally increases with the tip clearance because the flow velocity inside the cavity near the vertical squealer increases with the tip clearance."